Engine Air-Fuel Ratio and Torque Control using Secondary Throttles

A. G. Stefanopoulou,* J. W. Grizzle* and J. S. Freudenberg*

Abstract

A control scheme is designed to limit air-fuel ratio excursions and track driver-demanded torque for a 4-cylinder engine during rapid changes in throttle position. The new control scheme is based on joint management of air and fuel flow into the cylinders using secondary throttles placed before the intake ports of the cylinders, in combination with standard fuel injectors.

1 Introduction

Environmental regulations continue to drive research on improved vehicle emissions and fuel economy. The goal is to achieve cleaner burning and more efficient automobiles, without compromising driveability. This requires precise air-fuel ratio (A/F) control, both in steady state and in transient engine operation. A challenging problem for the Control Automotive Engineer is to keep the A/F close to stoichiometry during rapid changes in throttle position. Rapid changes in throttle position strongly influence the cylinder air charging process, mixture formation and transient performance of the engine. These rapid throttle movements reflect the driver's demand for changes in torque and vehicle acceleration.

The goal of the current work is to keep the A/F close to stoichiometry so that the Three Way Catalyst (TWC) operates with high efficiency, and to track the driver's torque demand during rapid changes in throttle position. The torque set point to be achieved is a function of throttle position and engine speed. This function, when evaluated for all possible throttle positions and engine speeds, forms a nonlinear map, called the "demand map".

The control of the A/F around stoichiometry is usually based on regulating the fuel flow to follow the air flow changes imposed by the driver. The associated feedback control system does not have high enough bandwidth to accommodate fast transients seen in normal driving due primarily to the long delay in the induction-compression-combustion-exhaust cycle, plus the transport delay in the

exhaust manifold. The addition of a feedforward term for the fuel set-point does not completely alleviate this problem. Developments in the area of drive-by-wire (DBW) throttle systems [5] have indicated the need for an air control scheme in addition to the fuel control, but have also originated questions on safety issues. In [2], a DBW throttle system has been used as a way of regulating (in the sense of predictability) the changes in air flow into the manifold caused by movements of the primary throttle. The present work moves a step beyond the DBW scheme by developing a joint air-fuel management system.

The control scheme presented here is based on the introduction of secondary throttles before the intake ports of the cylinders (Fig. 1). The new control surfaces (θ_c) regulate the air flow into the cylinders. These control surfaces in combination with the fuel injectors (F_c) achieve low A/F excursions and good tracking of torque demand by adjusting the air flow and the fuel flow into the cylinders. The control surfaces θ_c smooth out rapid changes of the charging process during throttle movements so that the fuel control path is able to maintain stoichiometry.
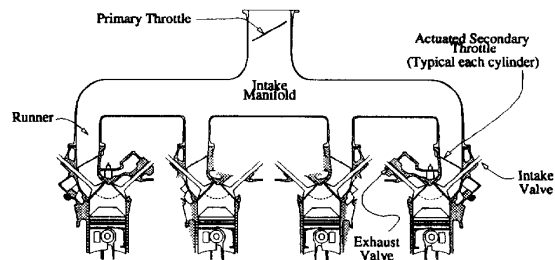
Figure 1: Schematic representation of 4-cylinder engine with secondary throttles.

The torque and A/F errors used by the controller are calculated by measuring the difference between actual and desired values. For now we are assuming direct measurement of the achieved torque; we have also used a linear EGO sensor for the estimation of the A/F from the exhaust gas. The engine model used in this study is a continuous-time nonlinear, low-frequency, phenomenological model with uniform pulse homogeneous charge and a lumped parameter approximation of the breathing and

rotational dynamics [3].

Definition of the variables and their units is provided in the next section. An overview of the model is given in Section 3. Section 4 discusses the dynamics of the nonlinear breathing process after the introduction of the secondary throttles; the nonlinear feedforward design of the set points for the secondary throttles is discussed in Section 5. The relationship between the primary throttle position and the torque set-point for the control scheme is described in Section 6. The linear feedback design, results and comparisons are given in Section 7. Conclusions and future work are discussed in Section 8.

2   Nomenclature

A/F	air-fuel ratio, unitless
$\dot{m}$	mass flow, g/sec
N	flywheel speed, rad/sec
P	pressure, bar
T_q	torque, Nm
θ	primary throttle position, degrees
θ_c	secondary throttle position, unitless $(0 \div 1)$

3   Engine Model

This section gives a brief overview of the nonlinear mathematical representation of the engine model used in our study (see Fig 2). For the complete dynamic equations describing the primary throttle body, the engine pumping and the torque generation, the reader is referred to the original paper [3]. A full description of the rotational dynamics as a function of the total inertia and the load torque is given in [6].

Figure 2: Engine model with secondary throttles.

The discrete nature of the combustion process causes delays in the signal paths: between the mass charge formation and the torque generation there exists a delay equal to the compression stroke duration, and between the exhaust manifold and the EGO sensor there exists a delay which equals 3 times the intake event duration. The dynamics of the exhaust manifold and the linear EGO sensor are modeled by first order differential equations with time constants equal to 0.15 sec and 0.20 sec respectively. The model of the fuel puddling dynamics is given in [1]

by

$$\dot{M}_f = \frac{0.62 \cdot s + 1}{0.1 \cdot s + 1} M_{fi}$$

where $\dot{M}_{fi}$: injected fuel flow (g/sec)

$\dot{M}_f$: cylinder port fuel mass flow (g/sec)

(3.1)

Precise transient air-fuel ratio control during rapid changes in the throttle position by the driver, requires feed-forward computation of the fuel injector pulse width since the inherent delay in the air-fuel ratio feedback loop prohibits rapid corrections. The fuel injector pulse width is regulated on the basis of the estimated cylinder air charge. The cylinder air charge is calculated by the estimated air flow rate out of the intake manifold multiplied by the duration of the intake event [7]. The dynamics of the air flow meter are included in the model by a first order lag with a time constant of 0.13 sec. Finally, fuel injection is often timed to occur on a closed-valve prior to the induction event [7]; this inherent delay has not been included in the model at this time.

4   Nonlinear Breathing Process

This section concentrates on the nonlinear dynamics of the engine breathing process. The study of the breathing process behavior is used to investigate and determine the operating regions where the secondary throttles (θ_c) have control authority in regulating the air charge into the cylinders. The air charge for every intake event is a function of the mass air flow rate into the cylinders and the engine speed, and it is directly related to the torque produced throughout the power stroke. Control over the transient and the steady state value of the mass air flow is necessary to meet the objectives of good torque tracking and maintaining the A/F at stoichiometry. The signal θ_c must influence the static and dynamic behavior of the manifold pressure, the air flow into the manifold through the primary throttle position, and the air flow into the cylinders through the secondary throttles.

The manifold acts as a plenum, where the rate of change of the manifold pressure (P_m) is proportional to the mass air flow rate into the manifold $(\dot{m}_\theta)$ minus the pumping mass air flow rate $(\dot{m}_f)$ into the cylinders. The manifold dynamics are described by the following first order differential equation (see [12]) that relates the rate of change of the manifold pressure (P_m) to the flow rates into and out of the manifold $(\dot{m}_\theta$ and $\dot{m}_f$ respectively)

$$\frac{d}{dt}P_m = K_m(\dot{m}_\theta - \dot{m}_f), \text{ where } K_m = \frac{R \cdot T}{V_m} \qquad (4.1)$$

The mass air flow rate into the manifold $(\dot{m}_\theta)$ through the primary throttle body is a function of throttle angle (θ), the upstream pressure (P_o), which we assume to be standard atmospheric, i.e. $P_o = 1$ bar, and the downstream pressure, which is the manifold pressure (P_m). When the manifold pressure is less than half of atmospheric pressure, i.e. $P_m/P_o < 0.5$, the flow $\dot{m}_\theta$ through the throttle body is described as sonic flow and depends only on the

primary throttle position. The function describing $\dot{m}_\theta$ in the two flow regimes is given in [11], and [13] by

$$\dot{m}_\theta = f(\theta)g(P_m)$$
$$f(\theta) = 2.821 - 0.05231\theta + 0.10299\theta^2 - 0.00063\theta^3$$
$$g(P_m) = \begin{cases} 1 & \text{if } P_m \le P_O/2 \\ \frac{2}{P_O}\sqrt{P_m P_O - P_m^2} & \text{if } P_m > P_O/2 \end{cases}$$
$$(4.2)$$

The engine pumping mass air flow rate ($\dot{m}_f$) is a function of manifold pressure (P_m) and engine speed (N) and is given in [3] by

$$\dot{m}_f = -0.366 + 0.008979 N P_m - 0.0337 N P_m^2 + 0.0001 N^2 P_m$$
$$(4.3)$$

For the basic model (without the secondary throttles) the steady state operating point occurs at the intersection of the two trajectories of the mass air flow rates. This point is the nominal point shown in Figure 3. With the introduction of the secondary throttles it is possible to scale the engine pumping rate ($\dot{m}_f$) by different values depending upon the effective area of the passage that is regulated by opening and closing these new valves:

$$\dot{m}_{cyl} = \theta_c \cdot \dot{m}_f. \qquad (4.4)$$

Figure 3 shows the new trajectories of the air flow rate into the cylinders and the resulting new equilibriums (set points in Fig. 3) for the breathing process. For sufficiently large $\theta_c < 1$, the steady state value of the mass air flow into the cylinder $\dot{m}_{cyl}$ is adjusted by causing the new equilibrium to shift from the sonic flow regime to the subsonic region. A closer investigation of the two regimes illuminates their significance in the new control scheme.
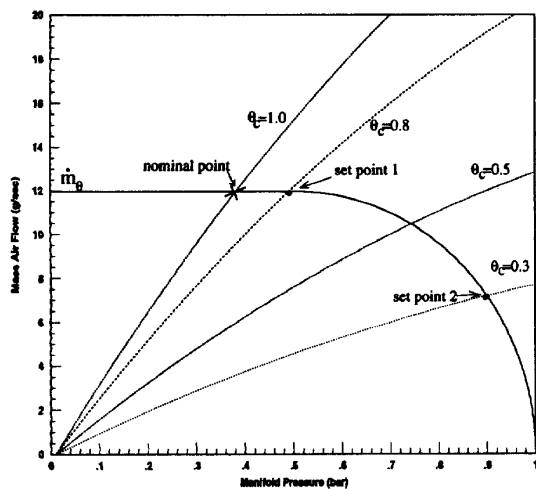
Figure 3: Trajectories of $\dot{m}_\theta$ and $\dot{m}_{cyl}$ for several values of θ_c.

When the flow through the primary throttle body is sonic and therefore does not depend on the manifold pressure, we operate in the flat region of $\dot{m}_\theta$ in Figure 3. Small changes in θ_c cause no change in the steady state value of

the mass air flow in and out of the manifold. For this reason, when the model of the breathing process is linearized, the secondary throttles have zero control authority on regulating the steady state mass air flow into the cylinders. This can be shown by the following transfer function between the control signal $\Delta\theta_c$ and the mass air flow into the cylinder $\Delta\dot{m}_{cyl}$:

$$\frac{\Delta\dot{m}_{cyl}}{\Delta\theta_c} = \frac{1}{1 + \frac{k_m k_1}{s}} = \frac{s}{s + k_m k_1} \qquad (4.5)$$

The DC gain of the above transfer function is clearly zero. The usual technique of incorporating an integrator to regulate the steady state mass air flow into the cylinders cannot be used here, since the transfer function has a zero at the origin that cancels the integrator pole. It is also instructive to see this on a block diagram level. Figure 4 shows the linear dynamics of the breathing process for sonic flow after the introduction of the secondary throttle. Note that the integrator loop, which is an intrinsic part of the manifold dynamics in sonic flow, rejects the signal θ_c in steady state. Thus the control signal $\Delta\theta_c$ cannot adjust the air charge into the cylinder by "smoothing" the effect of rapid throttle changes. Consequently, the control command $\Delta\theta_c$ has zero control authority on the A/F and the steady state value of the engine torque.
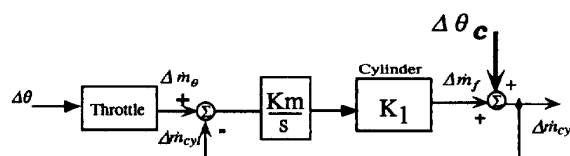

Figure 4: Block diagram of the linearized breathing process.

In the case where the flow is subsonic, i.e. $P_m/P_o > 0.5$, the air flow into the manifold depends on the primary throttle position and on the manifold pressure; thus the linear model of the engine breathing process is different from the above and the application of linear techniques is possible. The slope of the function that describes $\dot{m}_\theta$ (see Fig. 3) indicates the control authority of its opearting point. It is clear now that the control authority of the secondary throttles around the set-point 2 in Figure 3 is preferable to that around the set-point 1. Around set-point 2, the secondary throttles can be used to "smooth" any abrupt changes in air flow by regulating the air flow into the cylinders at a slower rate.

In conclusion, a nonlinear feedforward design of the θ_c set-points that allows operation in the subsonic flow regime, where the secondary throttle have maximal control authority, is necessary. This map will provide the steady state position of the new control surfaces.

5   Feedforward Control Design

The natural nominal position of the secondary throttles is wide open, i.e. $\theta_c = 1$. However, recall from Section

4 that under these conditions the secondary throttles often have zero control authority in adjusting the steady state value of the mass air flow into the cylinders. This paper proposes a solution that uses a control signal (θ_c), which consists of a nonlinear feedforward term ($\theta_{c_{fw}}$) plus a feedback term ($\theta_{c_{fb}}$). The feedforward design ensures maximal control authority and smooth engine operation. The feedback design is based on an LQG/LTR compensator.

The nonlinear feedforward term ($\theta_{c_{fw}}$) is designed to satisfy the following three conditions: 1) it is a smooth and non-decreasing function of the primary throttle position (θ) and the engine speed (N), i.e. $\theta_{c_{fw}} = \theta_{c_{fw}}(\theta, N)$; 2) the engine should deliver its maximum power output when operated at or close to wide open throttle (WOT), and 3) maximal control authority should be available without sacrificing combustion stability and performance. To achieve these objectives over a wide range of engine operating conditions we should consider the effects of combustion stability, thermodynamic performance indices and idle operating conditions. Presently we have not completed such an extended analysis, which we hope the results of this paper will initiate. Based only on a controllability analysis, we have developed the following map (see Fig. 5):

$$\theta_{c_{fw}} = \begin{cases} 0.55 & \text{if } 0^o < \theta < 12^o \\ 0.6445 - 0.0126 \cdot \theta \\ +1.3125 \cdot 10^{-4} \cdot \theta^2 \\ +2.1875 \cdot 10^{-5} \cdot \theta^3 & \text{if } 12^o \leq \theta < 20^o \\ 1 - \left(\frac{\theta - 60}{65}\right)^2 & \text{if } 20^o \leq \theta < 60^o \\ 1 & \text{if } 60^o \leq \theta < 90^o \end{cases}$$
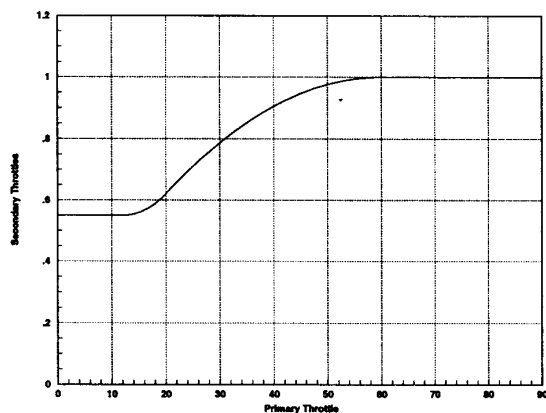
Figure 5: Static feedforward nonlinear term of the control signal θ_c

The reasoning behind this map is briefly explained. First of all, usual driving conditions in urban areas correspond to partly open primary throttle (θ) interrupted by rapid requests for acceleration and deceleration (which are the main causes of A/F excursion). At partly open throttle, the maximum power of the engine is not required and hence $\theta_{c_{fw}} < 1$ is acceptable. In addition, $\theta_{c_{fw}}$ has

been adjusted to ensure that the breathing process is operating near set-point 2 in Fig. 3. When the primary throttle is at or near WOT, the secondary throttles must smoothly operate close to the wide open position to ensure that maximum engine output can be achieved. Under WOT conditions, $P_m/P_o \approx 1$. Therefore the secondary throttles are operating in the maximal control authority region. However, they have freedom of movement only towards one direction. They can reduce the passage of the inlet runners and regulate the transient air flow rate into the cylinders during acceleration to cause lower A/F excursions. On the other hand, not much can be done when the driver closes the primary throttle: the secondary throttles cannot open further ($0 < \theta_c \leq 1$) to "smooth" the abrupt decrease of the air flow into the manifold by providing additional air. Finally, when the primary throttle is nearly closed, there is a minimum position for the secondary throttles below which idle stability issues have to be addressed.

In the present work, we use the above map to investigate the contribution of the new control actuator to driveability improvement and emissions reduction. Thermodynamic evaluation is needed to determine the interaction of the new control surfaces with the various engine performance indices. An initial assessment of the influence of the suggested feedforward scheme shows that the feedforward term is beneficial to the manifold dynamics. The engine operates at $P_m/P_o \approx 0.9$, i.e. manifold almost fully charged, which causes considerably faster manifold filling dynamics during part throttle driving. Achieving fast quasi-steady conditions close to atmospheric pressure in the intake manifold can eliminate wide variation in the time constant of the fuel puddling dynamics. This might reduce the uncertainty inherent in the fuel flow transient behavior. We also expect a reduction of the pumping losses due to low manifold vacuum . However, the additional complication in the intake system of the engine might decrease the volumetric efficiency. Further investigation of all the above issues will determine the effect of the new control scheme on fuel economy.

Usage of the feedforward term shown in Fig. 5 makes linearization fruitful. The Section 7 describes the linear feedback design for the secondary throttles and the fuel injectors.

6 Demand Map

In the proposed control scheme, the primary throttle position is the input. It is measured but not controlled. The torque set-point is calculated from the primary throttle position and the engine speed measurements. This requires a demand map, similar to the one used in DBW schemes [5], to determine the torque set-point for any throttle position and engine speed. The engine model, after the introduction of the feedforward term of the secondary throttles was used to create the nonlinear static map. The torque from the demand map will be used as

the desired torque when the torque error is calculated to adjust the control signals.

7 Simulation Example

The purpose of this example is to illustrate some of the properties of the closed loop system using the secondary throttles. The operating point about which we chose to linearize the engine model lies in the acceleration curve of the engine and third gear was used in the power-train rotational dynamics. The nominal primary throttle position used was $\theta = 20°$, and the nominal set-point for the secondary throttles was 61% open, resulting in a manifold pressure of $P_m = 0.96$ bar. The air flow into the cylinders was 15.4 g/sec at 3000 RPM producing 31.5 Nm of torque. The same amount of torque is produced by the conventional engine at a primary throttle position of $\theta = 11.8°$, with a manifold pressure of 0.51 bar. Note that this operating point falls into the low control authority region explained in Section 4. The resulting linear model has 10 states and is augmented with the two integrated states of the A/F and torque error.

The closed loop performance of the engine with the secondary throttles (θ_c-scheme) is compared with the conventional A/F control scheme (F_c-scheme) and with a DBW throttle scheme (DBW-scheme). The conventional A/F control scheme regulates the fuel pulse-width duration usually with a PI controller. Seeking a fair comparison between the conventional and the proposed controller, the conventional fuel pulsewidth duration regulation is designed based on an LQG/LTR controller. Both A/F and torque measurements are used to improve the estimation process. The DBW throttle system is designed to track the demanded torque and regulate A/F to stoichiometry. The multivariable control law used is based on LQG/LTR design methodology.

Figure 6 is a simulation of the nominal response of the θ_c-scheme and the F_c-scheme for a 10% step change in primary throttle position, which corresponds to 16% step change in torque demand. The θ_c-scheme has $\pm 0.14\%$ A/F excursion and essentially zero A/F and torque error after 50 intake events. The integrated error of A/F during a rapid throttle movement can be used as a measurement of engine emissions during that period. The integrated error of A/F for the F_c-scheme is 0.0402 and for the θ_c-scheme is 0.0051, which indicates a possible reduction of engine emissions. Also, the engine reaches the specified torque faster than in the F_c-scheme, improving driveability significantly. Note that the conventional fuel pulsewidth duration control does not affect the torque performance of the engine.

The simulation in Fig. 7 demonstrates the torque traking performance of the proposed scheme in comparison with the DBW-scheme. The emissions performance is equivalent in the two systems. The integrated A/F error (during one of the throttle step changes pictured in Fig 7) in the θ_c-scheme is 60% less than that in the
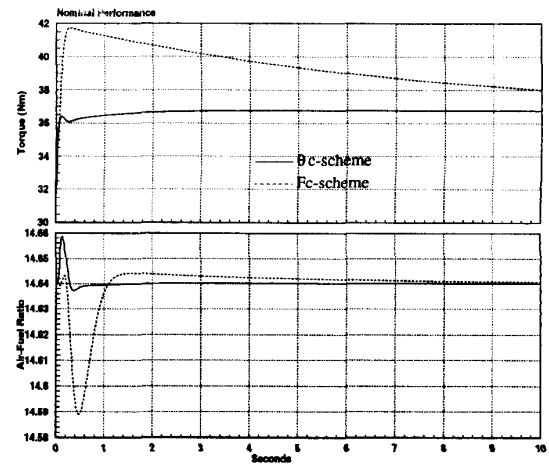

Figure 6: Simulation of the θ_c-scheme and F_c-scheme.

DBW-scheme. Though both responses are well within the high-efficiency window of the catalyst, the absence of the lean spike in the A/F in tip-in conditions in the DBW-scheme is immediately noticable. In DBW throttle systems, the engine is decoupled from the disturbances caused by the rapid throttle movements which are imposed by the driver. The closed loop system has the feature of isolating the high bandwidth torque demands by breaking the linkage between the driver and the primary throttles, facilitating smooth A/F control during transient engine operation. To achieve the same good A/F results we will need to form a smoother torque response in the engine. In the future we will incorporate the trade-off between the fast torque response and the small A/F excursion in the control design for the secondary throttles.
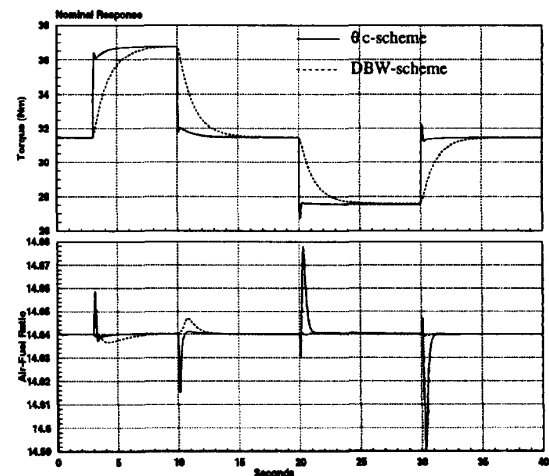

Figure 7: Closed loop response of the θ_c-scheme and DBW-scheme for a square wave in the demanded torque.

The performance of the θ_c-scheme was also tested un-

DOCKET ALARM

Explore Litigation Insights

Docket Alarm provides insights to develop a more informed litigation strategy and the peace of mind of knowing you're on top of things.

Real-Time Litigation Alerts

Keep your litigation team up-to-date with **real-time alerts** and advanced team management tools built for the enterprise, all while greatly reducing PACER spend.

Our comprehensive service means we can handle Federal, State, and Administrative courts across the country.

Advanced Docket Research

With over 230 million records, Docket Alarm's cloud-native docket research platform finds what other services can't. Coverage includes Federal, State, plus PTAB, TTAB, ITC and NLRB decisions, all in one place.

Identify arguments that have been successful in the past with full text, pinpoint searching. Link to case law cited within any court document via Fastcase.

Analytics At Your Fingertips

Learn what happened the last time a particular judge, opposing counsel or company faced cases similar to yours.

Advanced out-of-the-box PTAB and TTAB analytics are always at your fingertips.

API

Docket Alarm offers a powerful API (application programming interface) to developers that want to integrate case filings into their apps.

LAW FIRMS
Build custom dashboards for your attorneys and clients with live data direct from the court.

Automate many repetitive legal tasks like conflict checks, document management, and marketing.

FINANCIAL INSTITUTIONS
Litigation and bankruptcy checks for companies and debtors.

E-DISCOVERY AND LEGAL VENDORS
Sync your system to PACER to automate legal marketing.

fastcase®
Smarter legal research.